Quest Journals
Journal of Research in Mechanical Engineering
Volume 8 ~ Issue 2 (2022) pp: 23-36
ISSN(Online) : 2321-8185
www.questjournals.org

Research Paper

The Interplay Between an Edge Crack and a Parallel Internal Crack in an Infinite Sheet Under In-Plane Bending

Qin Ma[1], Mordechai Perl[2] and Cesar Levy[3*]
[1]*Edward F. Cross School of Engineering, Walla Walla University, College Place, WA 99324 USA*
[2]*Pearlstone Center for Aeronautical Engineering Studies, Dept. of Mechanical Engineering, Ben Gurion University of the Negev, Beer Sheva 84105 ISRAEL*
[3]*Dept. of Mechanical and Materials Engineering, Florida International University, Miami, FL 33199 USA*

ABSTRACT : *Non-destructive tests have found, in many cases, non-aligned parallel cracks in various in-service mechanical components. In such situations, any on-site evaluation requires an assessment of whether the cracks can be assumed coalesced or separate multiple cracks, for the application of Fitness-for-Service criteria. How to apply the criteria to non-aligned cracks is different depending on the source used. These standards are normally not determined in a rigorous and systematic way, and so can result in different outcomes. This observation is the reason for this study, namely, to investigate the stress intensity factor (SIF) of an edge crack in a 2-D finite sheet under pure bending, in the presence of a nearby parallel crack. The various crack alignment criteria found in the literature will be used to compare the results of the multiple aligned crack simulation for the purpose of recommending the conservativeness or non-conservativeness of the criteria as applied to the Fitness-for-Service situation. A 2-D linear elastic fracture mechanics (LEFM) analysis is undertaken of to characterize the interplay characteristic of the internal crack on the SIFs of the edge crack. The SIFs are evaluated as a function of the vertical and horizontal separation distances between the cracks,* ***S*** *and* ***H****, respectively; and as a function of the crack lengths of the edge crack and the internal crack given by* $\boldsymbol{a_2}$ *and* $\boldsymbol{a_1}$*, as well. The parallel cracks are assumed to be located in the region where the bending stresses are positive only. The SIFs have been obtained for dimensionless horizontal distances of* $\boldsymbol{S/a_2}$ *=0.4 to 2.0, and dimensionless vertical distances of* $\boldsymbol{H/a_2}$ *= -0.5 to 2.0. The investigation shows that certain crack alignment criteria are conservative compared to others, while certain crack alignment criteria provide inadequate information to be useful.*

KEYWORDS: *Non-aligned cracks, Fitness-for-Service, Edge crack, Internal Crack, Mixed Mode Behavior, Finite element, Stress Intensity Factors*

R*eceived 15 Feb, 2022;* ***R****evised 26 Feb, 2022;* ***A****ccepted 28 Feb, 2022 © The author(s) 2022.*
P*ublished with open access at* ***www.questjournals.org***

I. INTRODUCTION

When evaluating the diminished load bearing capacity of plant components, their failure is found to heavily depend on the simultaneous effect of multiple cracks on each other, the interplay characteristic, particularly when stress corrosion cracking (SCC) and fatigue are involved [1,2]. Fitness-for-Service (FFS) criteria employ an evaluation technique of multiple crack situations in order to determine the structural capacity of the cracked parts using fracture mechanics methodologies. If there are multiple cracks, they must be classified as to whether they exist on the same cross-sectional plane (aligned cracks) or not (unaligned cracks) using one of the crack alignment criteria. Various multi-crack alignment criteria have been proposed for on-the-job assessments. The criteria have been proposed in the American Society of Mechanical Engineers Boiler and Pressure Vessel Code Section XI (ASME Section XI) [3], Guide to methods for assessing the acceptability of cracks in metallic structures [4], European Fitness-for-Service Network (FITNET) [5], American Petroleum Institute (API) 579-1/ASME FFS-1 [6], and in Rules on Fitness-for-Service for Nuclear Power Plant Components in the Japan Society of Mechanical Engineers (JSME, S NA1-2008) [7]. These criteria are

*Corresponding Author: Cesar Levy
Florida International University, Miami, FL, 33199 USA

different from one another and some of them may provide more conservative results than others while some lead to non-conservative evaluations.

In the recent past, investigations have delved into the topic of multiple unaligned cracks in cases where two unaligned parallel internal cracks were contained within an infinitely large steel sheet. Kamaya [8] looked into the growth of multiple interactive surface cracks via a combined use of numerical and experimental techniques. Hasegawa and his group [9] evaluated the interplay of two parallel internal unaligned cracks in the FFS case using linear elastic fracture mechanics (LEFM). In current investigations, Hasegawa and his group [10-12], Miyazaki and his group [13], and Suga and his group [14] evaluated the plastic failure behavior for unaligned cracks.

In the previous studies none evaluated the interplay characteristic between two cracks, where one of the cracks is an edge crack. Also, the preceding investigations, to include the work of Ma and his colleagues [15], addressing the interplay characteristic between an edge crack and an internal crack, evaluated cases under uniaxial tension load conditions only. However, there are situations where a crack under bending is commonplace. Investigations for a single edge crack loaded in pure bending were addressed by Tada [16]. The cases addressed by Tada only cover a sheet with an edge crack and those cases do not address the topic of Fitness-for-Service at all.

Due to the limited scope of the previously mentioned investigations, the purpose of this article is to evaluate the interplay characteristic of an internal crack on the fracture behavior of an edge crack in a very long half sheet of height 2h, and width b, under the loading regimen of pure bending. The stress intensity factor (SIF) at the tip of the edge crack is evaluated for various edge crack and internal crack lengths given by a2 and a1, respectively, and for a variety of dimensionless vertical and horizonal separation distances, H/a2 = 0.4 to 2.0 and S/a2 = -0.5 to 2.0 respectively (see Fig. 1)..

II. MATERIALS AND METHODS

1.1 Problem Statement

The sheet arrangement is provided in Fig. 1. Within the sheet is an edge crack and an internal crack and the sheet is subjected to an in-plane pure bending moment as indicated. The sheet's material is that of steel with Young's modulus E=200 GPa, with Poisson ratio $\nu=0.3$, and having a yield stress σ_y=304 MPa. A linear load distribution is applied as shown in Fig. 1 on the top and bottom surfaces, equivalent to the applied bending moment, M. The largest bending stress σ_b is taken to be 2kPa. The cracks are always kept horizontal and parallel in relation to one another. The sheet has a width, b, and a semi-height, h, an edge crack of length a_2, and an internal crack of length $2a_1$. The gap in the horizontal direction is given by S parallel to the crack plane, and the vertical gap between the cracks is given by H at right angles to the crack surfaces.

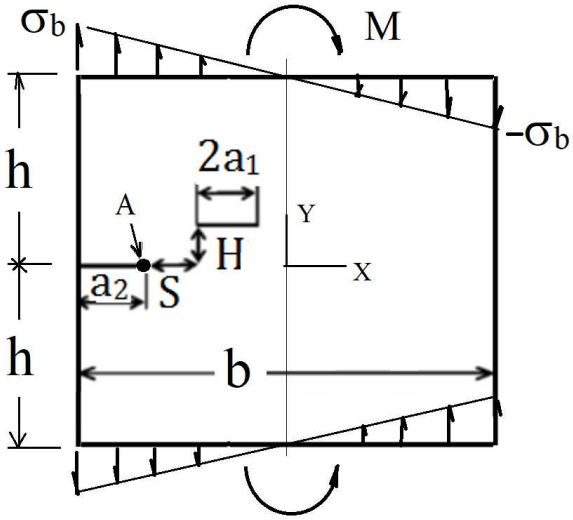

Figure. 1 A flat sheet with one edge crack and one parallel internal crack under pure in-plane bending. The separation distances S and H are defined and the location where the SIFs are calculated is identified as point A.

In all cases investigated, the sheet is assumed to be infinite so that the resulting bending moment varies in value depending on how the actual width dimension b is chosen. To eliminate size effects, the sheet's height

and width are chosen to be fifty times greater than to combined value obtained by adding the two crack sizes and the spacing between the cracks, namely $h=b=50*(a_1+S+a_2)$. Assuming the sheet thickness is 1, the bending stress σ_b is related to the applied moment M by:

$$M = \sigma_b \frac{t\,b^2}{6} \tag{1}$$

With the sheet thickness, t, is taken to be 1 to simplify the calculations. A typical calculation would look like this: If a_2=15mm, S=0 and $2a_1$=10mm, then b=50*(15+0+10) =1250mm =1.25m. This would produce an M=520.83 Nm. In the case where one crack is shorter, e.g., a_2=15mm, S=0, $2a_1$ = 5mm, then b =50*(15+0+5) =1000mm =1m. This would produce a moment, M=333.33 Nm, a smaller moment that would produce the same bending stress σ_b. The linear loading is applied so that the greatest bending stress, σ_b, is unchanged for all the finite element simulations undertaken. Further, the normalizing SIF used in our results, which depends on σ_b and a_2, will be constant. Its definition and usage are explained in the Results and Discussion section.

1.2 The Finite Element Model and its Validation

The SIFs at the edge crack tip A (see Fig. 1) are evaluated using the standard finite element (FE) code ANSYS APDL [17]. Most of the sheet is meshed using 2-D six-noded triangular elements. The elements are varied in size, small near the crack tip region and progressively increasing in size when farther away (see Fig. 2a). The region in the vicinity of crack tip a is meshed with singular elements (see Fig. 2b). The six-noded triangular element was employed as its quadratic displacement characteristic is applicable to model irregular meshes, specifically in the vicinity of the edge and internal crack in the infinite sheet.

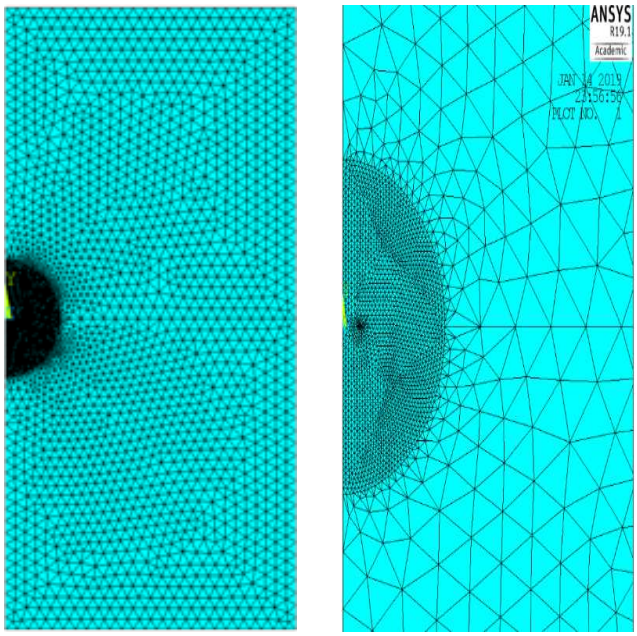

(a) (b)

Figure 2. The Finite Element Model: (a) a typical global mesh; (b) a typical mesh at the vicinity of the cracks

In the validation process of the finite element model, the Mode I SIF at tip A is used as a convergence criterion [15]. It was found that for meshes of more than 20000 degrees of freedom (DOF) the error is usually less than 3%. Therefore, in the present analyses typical meshes of 10000 elements with approximately 60000 DOFs are employed. The code option of automatic elements shape and aspect ratio adjustment was applied. To demonstrate the interplay characteristics between the two cracks, a typical von-Mises stress contour plot for the entire sheet is presented in Fig. 3a and a close-up of the crack-tip region is provided in Fig. 3b.

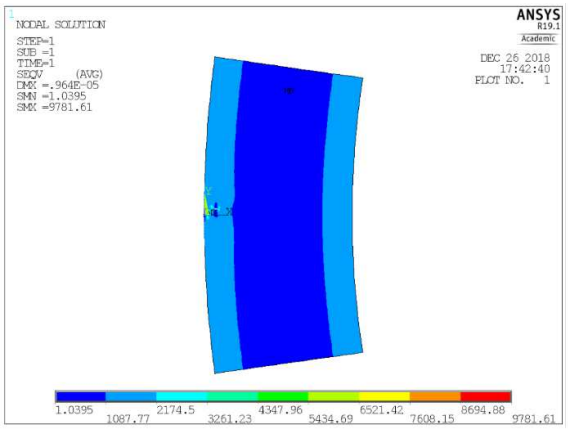

(a)

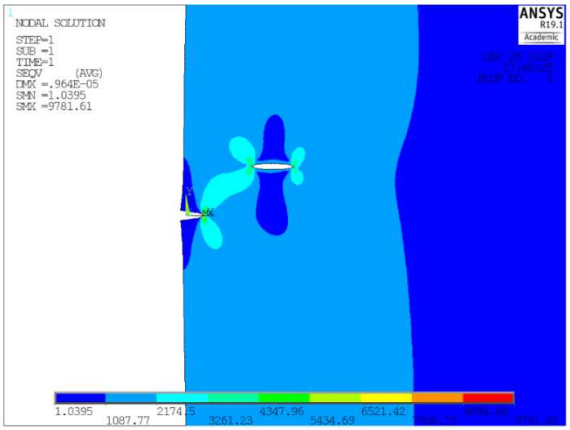

(b)

Figure 3. (a) A typical contour plot of von Mises stress of the sheet under pure bending, and (b) the von Mises stress at the vicinity of the cracks.

These two plots show the distinct interplay characteristic between the two cracks as well as the stress singularities at the tips of the two nonaligned cracks.

III. RESULTS AND DISCUSSION

3.1 Evaluation of the SIFs and their Normalization

The presence of the internal crack near to the edge crack results in a non-symmetric configuration. As a result, both cracks are loaded in Mixed Mode, and both K_{IA} and K_{IIA} exist at tip A of the edge crack. This Mixed Mode configuration produces a Mode II SIF which is no longer negligible when compared to the Mode I SIF. The ANSYS KCALC subroutine is used to obtain both Mode I and Mode II SIFs at tip A resulting from the remote bending moment (see [17] pp. 19-44 and onward). Normalization of the SIFs is accomplished via the factor K_0, namely:

$$K_0 = 1.12\,\sigma_b\sqrt{\pi a_2} \tag{2}$$

which is the SIF solution for a 2-D edge crack in an infinitely infinite sheet (Tada [16]) under a uniform tensile load of magnitude σ_b. This normalizing factor facilitates the comparison with the authors' previous investigation [15], and possibly with future results. In the present analysis, since σ_b and a_2 are kept constant, then K_0 is a constant; and, thus, the shapes of the normalized SIF graphs are representative of the actual SIF graphs and are not altered, only magnitudes are reduced.

3.2 Crack Spacing Effects on SIFs for Similar Size Cracks

The normalized Mode I SIF at tip A of the edge crack, due to the bending moment, K_{IA}/K_0, is given as a function of the dimensionless horizontal separation distance, S/a_2, for various values of the dimensionless

vertical separation distance, H/a_2. It is presented in Fig. 4 for the case of two cracks of similar size where a_2=15mm, $2a_1$=30mm and thus, a_1/a_2=1. The results in Fig. 4 point to the following conclusions:

a. The trends in Fig. 4 are found similar to those seen in cases evaluated for an infinite sheet under uniaxial tension for the same set of parameters [9, 15]. The normalized Mode I SIFs is found to be dependent on the dimensionless separation distances S/a_2 and H/a_2, as well as on the relative crack size, a_1/a_2.
b. The dimensionless Mode I SIFs of the edge crack, K_{IA}/K_0, increase when the cracks overlap ($S/a_2 < 0$), reaching a maximum, and then decrease as S/a_2 tends to 2.0. The magnitudes of the maxima depend on how close the cracks are vertically separated i.e., the smaller H/a_2 the higher the peak of K_{IA}/K_0.
c. The location of the maxima of the SIF depends on the vertical separation distance. As H/a_2 increases, the maximum of K_{IA}/K_0 occurs at larger values of S/a_2. For example, while for $H/a_2 = 0.4$ the maximum occurs at $S/a_2 \approx 0$, for $H/a_2 = 2.0$ it occurs at $S/a_2 \approx 1.4$. Furthermore, for $H/a_2 \geq 0.8$ the maxima always occur when $S/a_2 \geq 0$.
d. The rate of increase and decrease in K_{IA}/K_0 with the horizontal separation distance, S/a_2, is highly dependent on the vertical separation distance, H/a_2. The smaller H/a_2, the higher the rate of change of K_{IA}/K_0. For example, in the case of $H/a_2 = 0.4$, the peak value of K_{IA}/K_0 is 29% larger than the value at $S/a_2 = -0.5$. However, the maximum for the case of $H/a_2 = 2.0$, is only 8% higher than the value at $S/a_2 = -0.5$.
e. The significance of $S/a_2 \geq 0$ is that the cracks no longer overlap and continue to move farther away from each other, indicating at some point that the two cracks no longer show any interplay as the interplay characteristic has faded, i.e., they no longer "feel" each other's presence. In this case, the cracks can be treated as separate cracks in Fitness-for-Service considerations.

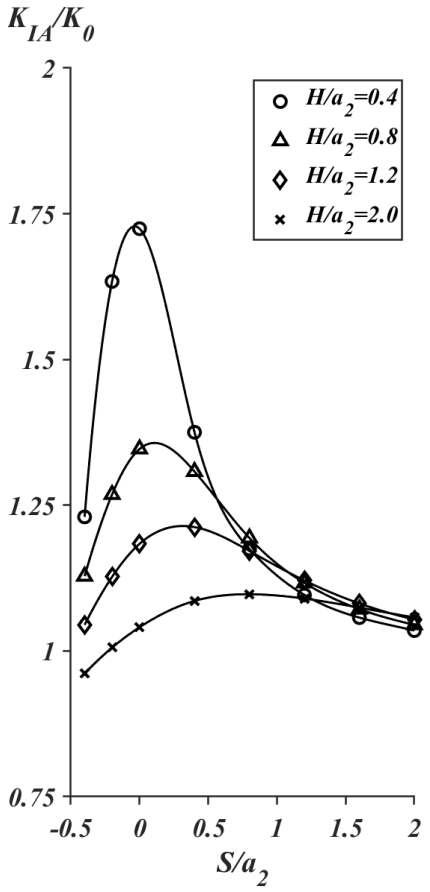

Figure 4. Normalized SIFs vs. S/a_2 as a function of H/a_2 for the edge crack-internal crack combination (a_2 = 15 mm; $2a_1$ = 30 mm).

Due to the non-symmetry of the problem, Mixed Mode conditions prevail at the tip of the edge crack. Figure 5 shows the relative importance of the Mode II SIF versus the Mode I SIF as the dimensionless

separation distance is varied both horizontally and vertically for the same case of a_2=15mm, $2a_1$=30mm and a_1/a_2=1.

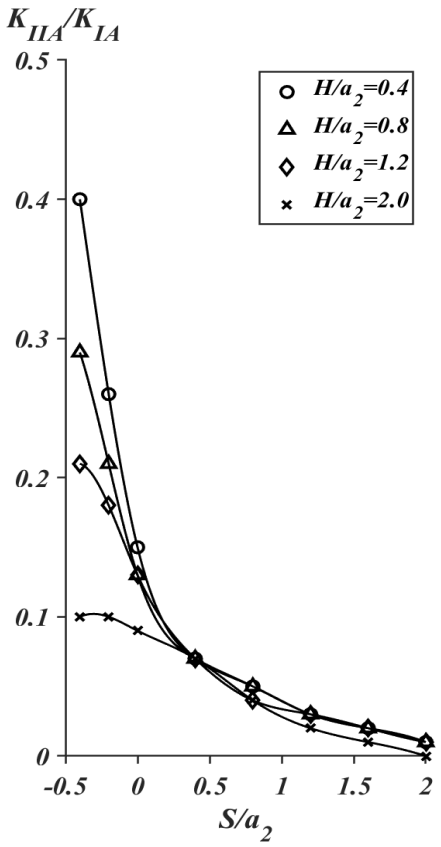

Figure 5. Mixed mode K_{IIA}/K_{IA} vs. S/a_2 as a function of H/a_2 for the edge crack-internal crack combination (a_2 = 15 mm; $2a_1$ = 30 mm).

The following conclusions can be drawn from the results shown in Fig. 5:

a. Under certain geometrical configurations, the internal crack may induce a considerable mode II SIF at the tip of the edge crack.
b. An example of (a) is if the critical value of K_{IIA}/K_{IA} is chosen to be 10%, then the Mixed Mode condition becomes important to the crack interplay characteristic. In such a situation, the Mode II SIF becomes significant for all the cases presented, i.e., when the two cracks overlap, and $S/a_2 < 0$. The higher the overlap between the two cracks, the higher the relative magnitude of K_{IIA}/K_{IA} and the greater becomes the importance of Mode II.
c. The largest Mode II SIF in this case is $K_{IIA}/K_{IA} \approx 0.40$ for $S/a_2 = -0.4$, and $H/a_2 = 0.4$.
d. To quantify the importance of a Mixed Mode evaluation in Fitness-for-Service analysis, a further theoretical/experimental study is necessary to provide the following data:
    1) How large is the energy release rate due to mode II (G_{II}), relatively to mode I (G_I)?
    2) What is the fracture toughness under mixed-mode conditions?
    3) What is the minimum value of K_{IIA}/K_{IA} above which a Mixed Mode analysis is significant?

It is worthwhile noting that, to date to the best of the authors' knowledge, a Mixed Mode analysis of two interacting parallel cracks in the context of Fitness-for-Service analysis has not appeared in print.

3.3 Crack Spacing Effects on SIFs for Dissimilar- Size Cracks

In this section the effect of shorter internal cracks on the SIF at the tip of the edge crack is evaluated for two values of internal crack length: $2a_1$=10mm and $2a_1$=5 mm. In the first case, while the edge crack length is kept the same as in the previous section, a_2=15mm, the internal crack is taken to be one-third the size,

$2a_1$=10mm, and thus, a_1/a_2=1/3. The results for this case for the same separation ranges as in Fig. 4, are presented in Fig. 6.

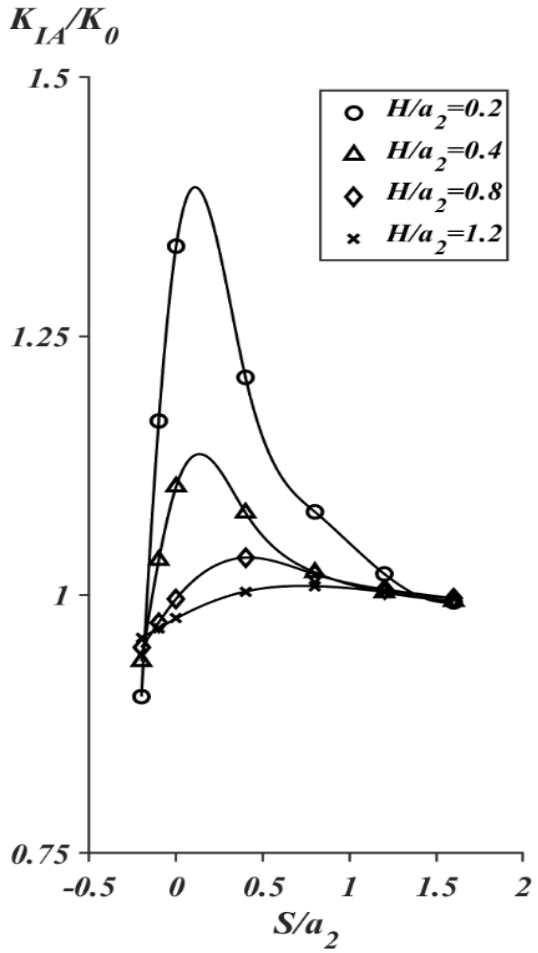

Figure 6. Normalized SIFs vs. S/a_2 as a function of H/a_2 for the edge crack-internal crack combination (a_2 = 15 mm; $2a_1$ = 10 mm).

The data in this case lead to the following conclusions:

a. Generally speaking, the pattern of the mode I SIF distributions in Fig. 6 is similar to that of Fig. 4, however the magnitudes are reduced. In the present case K_{IA}/K_0 =1.4 for the vertically closest case, H/a_2 =0.4, while in the previous case it was K_{IA}/K_0 =1.7 this is a reduction of about 18%. All the maxima are similarly reduced for all the values of H/a_2.
b. Shortening the internal cracks contracts the interaction range in terms of the horizontal separation distance. In the present case the interaction range is $\mathbf{0.5 \geq S/a_2 \geq -0.1}$ whereas in Fig. 4 it is $\mathbf{1.0 \geq S/a_2 \geq -0.4.}$

The impact of shortening the internal crack on the Mode II SIF for this case is demonstrated in Fig. 7. In this case a_2 = 15 mm; $2a_1$ = 10 mm and a_1/a_2=1/3. As in Fig. 6, the H/a_2 =0.2 graph is represented by the open circle icons, the H/a_2 = 0.4 graph is represented by the open triangle icons, the H/a_2 = 0.8 graph is given by the open diamond icons, and the H/a_2 = 1.2 graph is given by the cross icons.

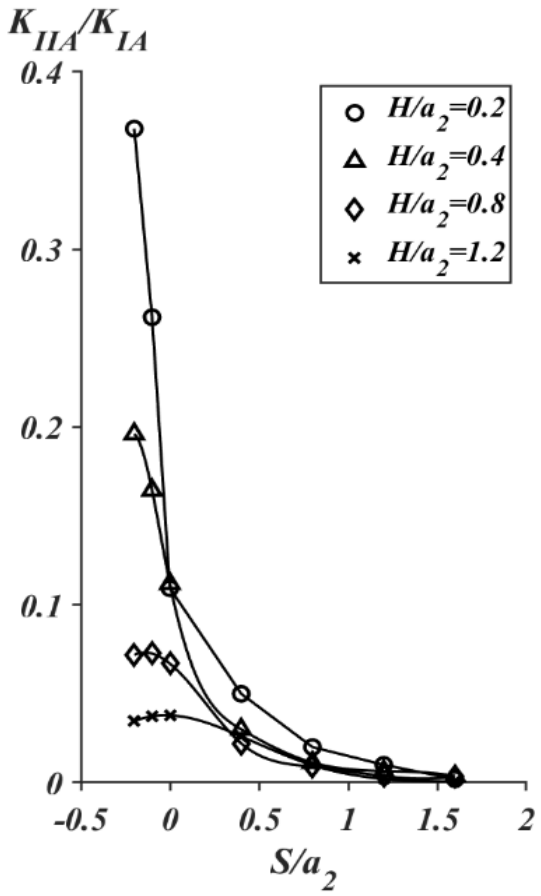

Figure 7. Mixed mode ratio K_{IIA}/K_{IA} vs. S/a_2 as a function of H/a_2 for the edge crack-internal crack combination (a_2 = 15 mm; $2a_1$ = 10 mm).

It is to be noted that the vertical separation distances treated in Fig. 7 are H/a_2 =0.2, 0.4, 0.8, and 1.2 while in Fig 5 H/a_2 = 0.4, 0.8, 1.2 and 2.0. Also, the horizontal distances treated in Fig. 7 are S/a_2 = -0.2, -0.1, 0.0, 0.4, 0.8, 1.2, and 1.6 while in Fig. 5 S/a_2 = -0.4, -0.2, 0.0, 0.4, 0.8, 1.2, 1.6 and 2.0. These changes are a result of the diminished interaction range between the cracks in which the interplay characteristic has an effect.

The effect of a shorter internal crack manifests itself in the following manner:

a. In both cases, of Fig. 5 and Fig. 7, the presence of the internal crack results in a significant Mode II SIF, as long as the cracks overlap $S/a_2 < 0$.
b. The Higher the overlap between the two cracks the higher the relative magnitude of K_{IIA}/K_{IA}, and the greater becomes the importance of Mode II.
c. For identical vertical separation distances, a shorter internal crack results in a smaller K_{IIA}/K_{IA}. For example, at S/a_2= -0.2, in the case of the shorter internal crack, K_{IIA}/K_{IA} is reduced by 25%, 64% and 80% for vertical separation distances of H/a_2=0.4, 0.8, and 1.2, respectively. Namely, the effect of the small internal crack on the edge crack is weaker, in this case, fading more rapidly as the vertical separation distance increases.
d. The largest Mode II SIF in this case is $K_{IIA}/K_{IA} \approx 0.37$ for S/a_2 = -0.2, and H/a_2 = 0.2
e. From the results in Fig. 5 and Fig. 7 it is evident that Mode I is still the dominant mode as the maximus K_{IIA}/K_{IA} is at most 0.4 in the cases studied.

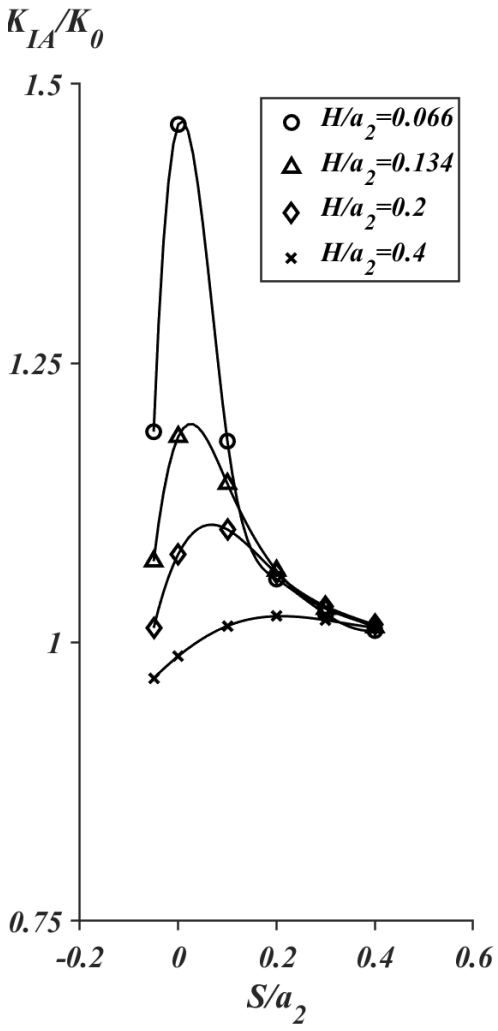

Figure 8. Normalized SIFs vs. S/a_2 as a function of H/a_2 for the edge crack-internal crack combination (a_2 = 15 mm; $2a_1$ = 5 mm).

In a second case of a very short internal crack, the length of the edge crack is still maintained as a_2=15mm. However, the very short internal crack is taken to be $2a_1$=5mm, with a relative crack size of a_1/a_2=1/6. The normalized Mode I SIFs, K_{IA}/K_0, for this case are presented in Fig. 8.

According to the results in Fig. 8, the following can be determined:

a. Comparing Figs. 4, 6, and 8, the shorter the internal crack, the weaker its effect on the SIF at tip A of the edge crack. Thus, the relative crack size a_1/a_2 is quite influential vis-à-vis the Mode I SIFs.
b. It appears that the two cracks must be very close vertically or very close horizontally for the two cracks to be considered as one, e.g., when H/a_2 = 0.066 or when S/a_2 = 0. These conclusions are consistent with the results reported in [15] for similar cases under uniaxial tension.

3.4 The Influence of Crack Alignment Rules

Although the geometrical configurations in all the cases presented herein are non-symmetric, the Mode I SIF is still dominant. Thus, the effect of different alignment criteria will be discussed under Mode I conditions to avoid added complexity.

The normalized Mode I SIFs of Fig. 4 are graphed in Fig. 9, overlaid by two curves representing two different Fitness-for-Service rules [4, 5]. The thick dark curve is the outcome of the British Standards crack alignment criteria [4] (labeled BritS), while the thick dotted-dashed curve is representative of the crack alignment criteria defined by FITNET [5] (labeled FFS).

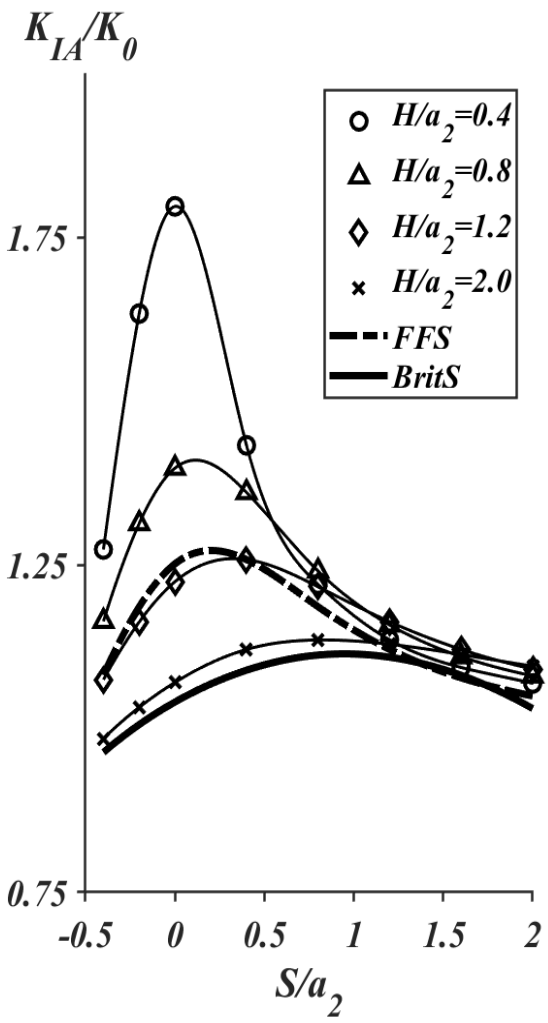

Figure 9. Normalized SIFs vs. S/a_2 as a function of H/a_2 for the edge crack-internal crack combination (a_2 = 15 mm; $2a_1$ = 30 mm) with FITNET standard (FFS) and British standards (BritS).

The BritS criterion is given by:

$$S_1 \leq a_1 + a_2 \tag{3}$$

where S_1 is the shortest distance between tip A of the edge crack and the internal crack tip closest to the edge crack tip.

The FITNET criterion is defined by

$$H \leq min(2a_1, a_2) \tag{4}$$

The British Standard (BritS) seems to account implicitly for the effect of both the normalized vertical and horizontal separation distances, H/a_2, and S/a_2, as well as the crack size ratio, a_1/a_2. The thin dashed curve is an outcome of that inequality and is derived from Eq. (3):

$$\frac{H}{a_2} \leq \sqrt{\left(\frac{a_1}{a_2}+1\right)^2 - \left(\frac{S}{a_2}\right)^2} \tag{5}$$

Hence, for a fixed a_1/a_2, as S/a_2 varies, each point on the thick dashed curve represents a different value of vertical separation distance, H/a_2. Therefore, the criterion involves all the dimensionless parameters S/a_2, H/a_2 and a_1/a_2.

In the case of the FITNET criterion the situation is different, as it does not involve the dimensionless horizontal separation, S/a_2, which is an important parameter that influences the SIF values. In fact, for the case presented in Fig. 9, the min ($2a_1$, a_2) is a_2 =15mm; hence, H/a_2 = 1. Thus, the thick dotted-dashed curve was determined under a relative separation distance H/a_2 = 1, with a_1=15mm, for various S/a_2 values using ANSYS in the same manner used to obtain the results for other cases.

The two criteria provide different outcomes in the determination of alignment vs. non-alignment for two parallel nonaligned cracks under bending. For certain crack separations, one criterion may suggest that the two cracks on parallel planes can be considered as coalesced, while the other criterion will suggest that the cracks should be treated as separate cracks, e.g., when S/a_2 = 0 and H/a_2 = 1.5. The critical values from the BritS and the FITNET criteria, as demonstrated in Fig. 9, unequivocally indicate that the FITNET provides a much higher hurdle for the cracks to be considered as coalesced [4, 5], especially when $S/a2 < 1$. Thus, the FITNET is a much more conservative rule. At the same time for the same range of S/a_2, the BritS provides lower critical values of the SIFs. It may thus, provide non-conservative results in Fitness-for-Service applications.

3.5 Crack Alignment Rules with Mixed Mode Effect Included

As mentioned previously, Mixed Mode effects cannot be neglected in many of the cases investigated. Therefore, a suggested methodology to integrate Mixed Mode situations into the Fitness-for-Service criterion would be to replace the use of the SIF in Fitness-for-Service calculations with the total energy release rate [16], namely:

$$G = G_I + G_{II} \tag{6}$$

where, by substitution, one obtains:

$$G = K_I^2/E' + K_{II}^2/E' \tag{7}$$

and where $E'=E$ for plane stress, and $E'= E/(1-\upsilon^2)$ for plane strain.

Defining an effective SIF to be used in the Fitness-for-Service criterion,

$$G=K_{Ieff}^2/E' \tag{8}$$

leads to the following definition of K_{Ieff}:

$$K_{Ieff}^2/E'=K_I^2/E'+K_{II}^2/E'=(K_I^2/E')*(1+[K_{II}/K_I]^2), \tag{9}$$

or

$$K_{Ieff}=K_I*(1+[K_{II}/K_I]^2)^{1/2} \tag{10}$$

Figure 10 investigates how Mixed Mode effects can be included in evaluating Fitness-for-Service criteria by employing K_{Ieff} in the case a_2 = 15 mm; $2a_1$ = 30 mm. The graph format used in Fig. 9 is applied here but the plots are those of K_{Ieff}/K_o versus S/a_2 for the same H/a_2 values. Again, K_{Ieff} is evaluated at point A in Fig. 1.

By comparison to Fig. 9, the FFS and the BritS plots of Fig. 10 have moved upward vis-à-vis the H/a_2 curves. By comparing the H/a_2 =2 curves of Figs. 9 and 10, we note that in Fig. 9 the curve was above the BritS curve, meaning the cracks are considered coalesced. Now, in Fig. 10, it is slightly below the BritS curve, meaning that the cracks are considered separate. This H/a_2 =2 curve is always below the FFS indicating that the cracks would be considered separate vis-à-vis that criterion.

By studying the the H/a_2 =1.2 curve in Fig. 9, it is noted that part is below, and part is above the FFS curve indicating that for $S/a_2 \leq 0.4$, the cracks are considered coalesced; beyond S/a_2=0.4 they are considered separated. In Fig. 10, it is noted that the H/a_2 =1.2 curve is below the FFS curve indicating that the cracks are considered separated. For this case, the BritS curve is below the H/a_2 =1.2 curve; thus, the cracks are considered coalesced vis-à-vis this criterion. Both the H/a_2 = 1.2 and 2 curves show how the introduction of Mixed Mode effects can have profound implications on the application of the Fitness-for-Service criteria.

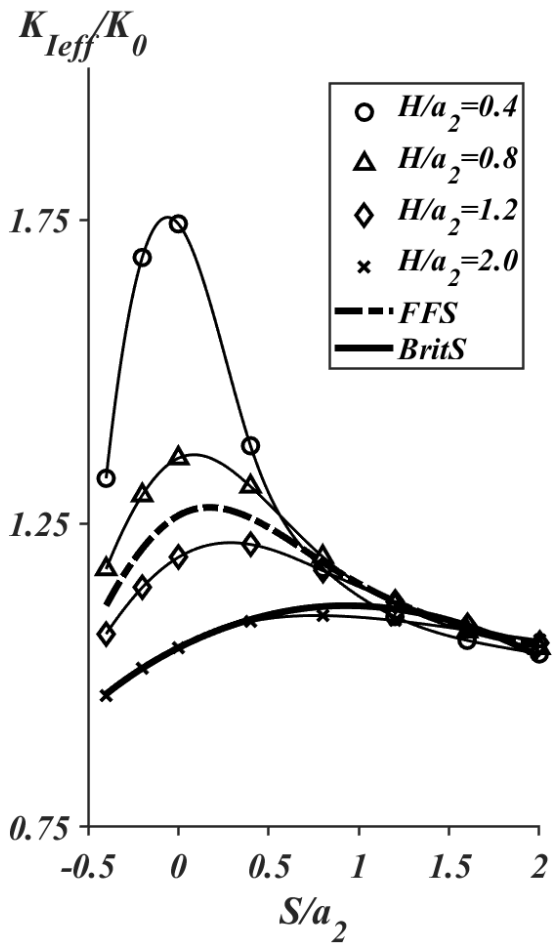

Figure 10. Normalized Mixed Mode effective SIFs vs. S/a_2 as a function of H/a_2 for the edge crack-internal crack combination (a_2 = 15 mm; $2a_1$ = 30 mm) with FITNET standard (FFS) and British standards (BritS).

IV. CONCLUSIONS

In this investigation, Mode I and Mode II SIFs at the tip of an edge crack under remote bending were determined when influenced by an internal crack lying on a parallel plane. The SIFs were found to be a function of the normalized vertical and horizontal separation distances as well as the relative crack sizes of the two cracks.

Below is a summary of the findings:

1. Due to the existence of an internal crack, the symmetry conditions of an edge-crack under pure bending is altered, resulting in mixed-mode conditions.
2. The relative resulting Mode II SIF, K_{IIA}/K_{IA}, may become considerable when the two cracks are overlapping. The greater the overlap, the larger K_{IIA}/K_{IA}.
3. K_{IA}, K_{IIA} as well as K_{IIA}/K_{IA} at the tip of the edge crack are found to be functions of the three dimensionless parameters: S/a_2, H/a_2, and a_1/a_2.
4. For any given vertical separation distance, the interplay characteristic of the cracks is limited to act within a certain range of the horizontal separation distance. This limited region is found to increase as the absolute crack size of the internal crack increases. It is believed that if the internal crack is fixed and the edge crack increases, the same behavior will be identified.
5. As the two cracks are separated further, whether in the vertical or in the horizontal direction,
6. the interplay characteristic fades, and the edge crack is practically under Mode I conditions.

7. The minimally addressed issue of Mixed Mode in the present analysis deserve further attention in Fitness-for-Service considerations.
8. The existing alignment rules, used to assess the "Fitness-for Service" of a component, do not agree and can lead to distinctly different conclusions, that may result in dangerous situations. More work needs to be done to bring these codes under one acceptable set of rules.
9. Mode II effects cannot be neglected in many of the cases investigated and can have serious implications on crack separation determination, as seen from the Fig. 9 and 10 comparisons.

ACKNOWLEDGMENTS

The first author (QM) would like to express his deep gratitude to Walla Walla University for its support through its Faculty Development Grant Fund 119290-12. There are no other sources of funding for this work. We acknowledge that a portion of this work was presented at the 2019 ASME PVP Conference in San Antonio, Texas, USA [18]. The authors thank ASME for allowing the modified and more comprehensive version of the paper to be published in this issue of the AIMS journal.

CONFLICT OF INTEREST

The authors declare that there are no conflicts of interest involved in this research work.

Appendix -- Nomenclature

a_1	-	half internal crack length
a_2	-	edge crack length
t	-	sheet thickness is taken as 1
b	-	sheet width
h	-	sheet height
H	-	vertical crack separation distance
S	-	horizontal crack separation distance
S_1	-	distance between edge crack tip and internal crack's closest crack tip
E	-	Young's modulus
E'	-	The value of E for plane stress or plane strain
G	-	total energy release ratee
G_I	-	Mode I energy release rate
G_{II}	-	Mode II energy release rate
K_I	-	Mode I SIF
K_{II}	-	Mode II SIF
K_{IA}	-	Mode I SIF at tip A of the edge crack (see Fig. 1)
K_{IIA}	-	Mode II SIF at tip A of the edge crack (see Fig. 1)
K_{Ieff}	-	the effective SIF (see Eq.
K_0	-	Normalizing SIF
M	-	Applied pure moment

Greek Symbols

v	-	Poisson's ratio
σ_b	-	Bending stress
σ_y	-	yield stress

REFERENCES

[1]. Okamura Y, Sakashita A, Fukuda T, et al. (2003) Latest SCC issues of core shroud and recirculation piping in Japanese BWRs. Transactions of the 17th International Conference on Structural Mechanics in Reactor Technology (SMIRT 17), Aug 17-22, 2003, Prague, Czech Republic, WG01-1.

[2]. Kamaya M, Haruna T (2006) Crack Initiation Model for Type 304 Stainless Steel in High Temperature Water. Corrosion Science 48: 2442–56. https://doi.org/10.1016/j.corsci.2005.09.015.

[3]. ASME (2007) ASME Boiler and Pressure Vessel Code, Section XI. Rules for inservice inspection and tests of nuclear power plant components. July 2007, New York: ASME International.

[4]. British Standards (2005) Guide to methods for assessing the acceptability of cracks in metallic structures BS 7910, London, UK: British Standards Institution.

[5]. FITNET (2001) European Fitness-for-Service Network, Proposal No. GTC1-2001-43049,Contract No. GIRTCT-2001-05071, www.eurofitnet.org

[6]. American Petroleum Institute (2007) Fitness-for-Service. American Petroleum Institute Standard API 579-1/ASME FFS-1, Washington, DC: API Publishing Services.

[7]. The Japan Society of Mechanical Engineers (2008) Rules on fitness-for-service for nuclear power plant. JSME S NA1-2008, Tokyo: JSME (in Japanese).

[8]. Kamaya M (2008) Growth evaluation of multiple interacting surface cracks. Part I: Experiments and simulation of coalesced crack. Eng Fract Mech 75: 1350–1366. https://doi.org/10.1016/j.engfracmech.2007.07.014.
[9]. Hasegawa K, Saito K, Miyazaki K (2009) Alignment Rule for Non-Aligned Flaws for Fitness-for Service Evaluations Based on LEFM. ASME JPVT 131: 041403. https://doi.org/10.1115/1.3152229.
[10]. Hasegawa K, Miyazaki K, Saito K (2010) Behavior of plastic collapse moments for pipes with two non-aligned flaws. ASME 2010 Pressure Vessels and Piping Division/K-PVP Conference, July 18-22, 2010, Bellevue, Washington, USA. https://doi.org/10.1115/PVP2010-25199.
[11]. Hasegawa K, Miyazaki K, Saito K (2011) Plastic collapse loads for flat plates with dissimilar non-aligned through-wall cracks. ASME 2011 Pressure Vessels and Piping Conference, July 17-21, 2011, Baltimore, Maryland, USA. https://doi.org/10.1115/PVP2011-57841.
[12]. Miyazaki K, Hasegawa K, Saito K (2011) Effect of flaw dimensions on ductile fracture behavior of non-aligned multiple flaws in a solid. ASME 2011 Pressure Vessels and Piping Conference, July 17-21, 2011, Baltimore, Maryland, USA. https://doi.org/10.1115/PVP2011-57559.
[13]. Suga K, Miyazaki K, Kawasaki S, et al. (2011) Study on the interaction of multiple cracks in ductile fracture process. ASME 2011 Pressure Vessels and Piping Conference, July 17-21, 2011, Baltimore, Maryland, USA. https://doi.org/10.1115/PVP2011-57188.
[14]. Suga K, Miyazaki K, Senda R, et al. (2011) Ductile fracture simulation of multiple surface flaws. ASME 2011 Pressure Vessels and Piping Conference, July 17-21, 2011, Baltimore, Maryland, USA. https://doi.org/10.1115/PVP2011-57147.
[15]. Ma Q, Levy C, Perl M (2013) A LEFM Based study on the interaction between an edge and an embedded parallel crack. ASME 2013 Pressure Vessels and Piping Conference, July 14-18, 2013, Paris, France. https://doi.org/10.1115/PVP2013-97083.
[16]. Tada H, Paris PC, and Irwin GR (2000) The Stress Analysis of Cracks Handbook, 3rd ed., New York: ASME.
[17]. Swanson Analysis System Inc. (2009) ANSYS 12 User Manual. Swanson Analysis System, Canonsburg, PA: SAS IP Inc.
[18]. Ma Q, Perl M, Levy C (2019) Stress intensity factors for an edge crack interacting with an embedded parallel crack for a finite plate under pure bending. ASME 2019 Pressure Vessels and Piping Conference, July 14-19, 2019, San Antonio, TX, USA. https://doi.org/10.1115/PVP2019-93248.